Advanced Carbon Journal, 2024, Vol. 1, Iss. 1, 93-110

DOI: 10.62184/acj.jacj1000202425

Review Article

SCIENCE PARK PUBLISHER

Advanced Carbon Journal

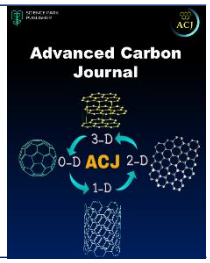

Effect of Carbon Nanostructures and Some Nanoparticles on (Cu, Tl)-1223 Phase Superconductor

Batool Jabbar Obaid AL Toofan[1,*], Shaker Ebrahim[1], Mohamed Anas[2], Ayman Mousa El Tahan[3], and Moustafa Mohammed Mahmoud Matar[2]

[1] Materials Science, Department of Materials Science, Institute of Graduate Studies and Research, Alexandria University

[2] Department of Physics, Faculty of Science, Alexandria University

[3] Department of Physics, Faculty of Science, Tanta University

Received: 06, 09, 2024; Accepted: 13, 10, 2024; Published: 08, 11, 2024

Abstract

Large-scale applications of high-temperature superconductors (HTSCs) require superconductors with high critical current density operating at 77 K in a strong magnetic field. However, some challenges are faced in large-scale applications such as strong superconducting anisotropy, their irreversible and critical current density values under high field at 77 K not high enough. In this review, the effect of different carbon nanostructures such as carbon nanotubes (CNTs), graphene, and graphene oxide on HTSCs was discussed. In addition, the effect of some metal and metal oxide nanoparticles on HTSCs was reviewed. It was noted that adding nanoparticles and quantum dots at lower concentrations to HTSCs is one of the most efficient ways to increase their critical current density and flux pinning.

Keywords: Carbon nanotubes; Graphene; Nanoparticles; (Cu, Tl)-1223 Phase; Superconductors

1. Introduction

A superconductor or ideal conductor is an electrical conductor with zero resistance. The material from which it is made has no resistance, but on the other hand, has superconductivity. This is an ideal principle in electrical engineering that cannot be reached at present, but it is used when the resistance of the conductor is small, so it is preferable to ignore it, as in the resistance of the connecting wires in an electrical circuit. A perfect superconductor has no electrical resistance and perfect diamagnetism when cooled below a certain temperature known as the superconducting transition temperature, "T_c", as shown in Figure (1-a) [1]. It acts as a metal at higher temperatures and is not a good conductor in most cases. However, some metals lead, tantalum, and tin produce superconductivity at T_c of 7.2, 4.47, and 3.7 K respectively. Some superconducting metals are mildly diamagnetic in the normal state above T_c, whereas others are paramagnetic. They have perfect electrical conductivity and excellent or noticeable diamagnetism below T_c. The second distinguishing diamagnetism of superconductors indicates that superconducting materials do not allow an externally applied magnetic field to enter their interior. This phenomenon is known as the "Meissner effect," as depicted in Figure (1-b) [2]. Superconductors can be categorized into two types. Type I superconductors are those that completely exclude applied magnetics flux, and the field where this occurs is known as the

Advanced Carbon Journal, 2024, Vol. 1, Iss. 1, 93-110

DOI: 10.62184/acj.jacj1000202425

critical magnetic field “Bc" as illustrated in Figure (2- a). The other superconductors, known as Type II superconductors, are similarly perfect conductors but have more intricate magnetic characteristics. As illustrated in Figure (1.2 b), this type of superconductor has two separate critical magnetic fields, designated by B_{c1} and B_{c2}. B_{c1} and B_{c2} are lower in the upper-critical magnetic field, respectively, with no magnetic flux density inside the sample for tiny amounts of applied magnetic field B, i.e. B = 0. However, once the field exceeds B_{c1} in type II superconductors, the magnetic flux starts to penetrate the superconductor and hence H ≠ 0 and M inside the material decreases to smaller values than the full Meissner value of –H. Above H_{c1} and below H_{c2} the substance is in the mixed state of flux which means superconducting state with cylinders of normal state. These cylinders or flux tubes are called vortices. Upon increasing the magnetic field H than H_{c2} the superconductivity is destroyed and M = 0 [2].

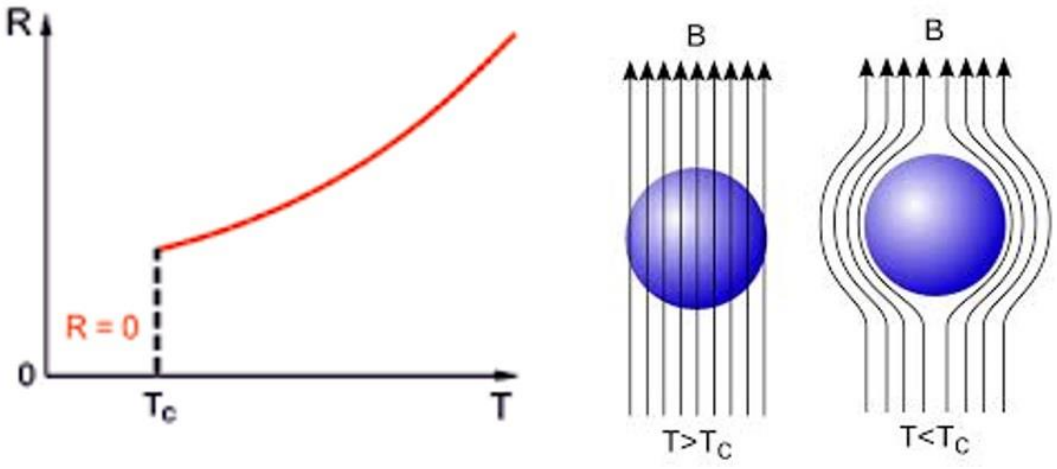

Figure 1. Superconductivity properties: (a) Zero resistivity and (b) Meissner effect.

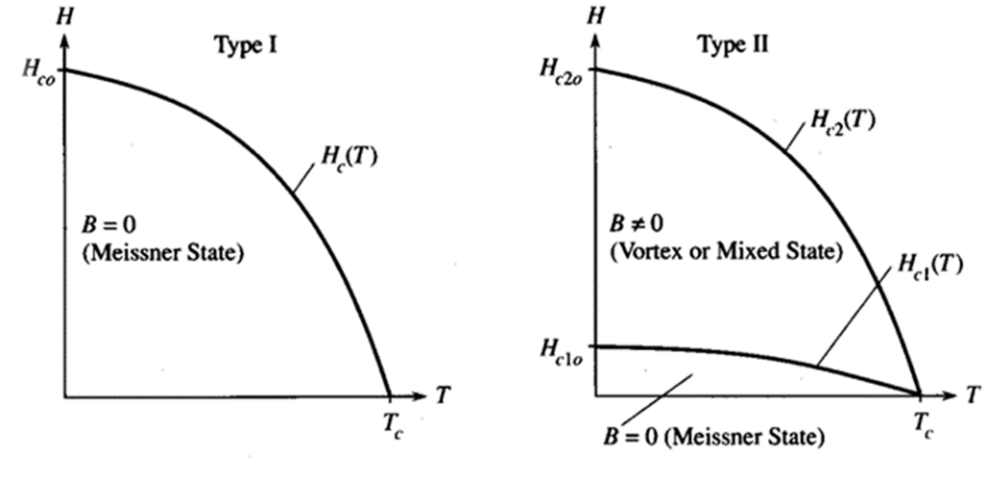

Figure 2. B-T phase diagram for (a) Type I and (b) Type II superconductors.

Advanced Carbon Journal, 2024, Vol. 1, Iss. 1, 93-110
DOI: 10.62184/acj.jacj1000202425

Review Article

Onnes began researching the electrical characteristics of metals at extremely low temperatures in 1911. Onnes reduced the temperature while passing a current through an extremely pure mercury wire and measuring its electrical resistance. The resistance abruptly vanished at 4.2 K and was equal to zero. According to Onnes, Hg has entered a new condition, which is known as the superconducting state [3-5]. Onnes found that Pb was a superconductor at 7.2 K in 1913. At T_c = 9.2 K, Nb required another 17 years to be found as a superconductive element [3, 4]. More than 2000 superconducting materials were discovered in 1975, and the superconducting transition temperature had reached 22.3 K with the discovery of A-15 compounds such as, Nb_3Ge, in 1973 [6-8]. Sleight et al. [9], reported in 1975 that superconductivity was seen in $BaPb_{(1-x)}Bi_xO_3$ and the superconducting transition temperature of this compound changes with the Bi/Pb ratio and reached the highest value of 13 K.

The alloy Nb_3Ge possessed the greatest superconducting transition temperature, Tc=23.2 K, until 1986. Early in 1986, Bednorz and Müller [8] discovered that a mixed-phase lanthanum, barium, and copper oxide in the form of a ceramic became superconducting at Tc = 30 K. At the University of Tokyo, Takagi et al. [10] showed that such superconducting temperature range of Ba-substituted La_2CuO_4 was just as high as 30 K by c the end of 1986. Lanthanum compound by the beginning of 1987 became superconductor at T_c = 40 K at ambient pressure [8, 10, 11] as well as up to 52 K at high pressure [11]. $La_3Ba_3Cu_6O_y$ systems demonstrated a superconducting transition temperature of Tc 80 K [12-17]. Chu et al. [18] discovered a novel superconducting material, $YBa_2Cu_3O_7$, with just a superconducting transition temperature exceeding 90 K in 1987. With the discovery of Bi-Sr-Ca-Cu-O [19, 20] in early 1988, the superconducting temperature range surpassed 110 K, followed by Tl-Ba-Ca-Cu-O [20-25]. In 1993, Berkly et al. [26] reported T_c=131.8 K for $Tl_2Ba_2Ca_2Cu_3O_{10-\delta}$ under a pressure of 7 GPa.

T_c exceeding 130 K has been recorded by several studies for such Hg-series of chemicals $HgBa_2Ca_nCu_{n+1}O_{2n+4}$ when n=1, 2, and 3 and sometimes with Pb-substitution for Hg [26, 27]. The temperature of Hg compounds superconducting transition raised with pressure and T_c values reached 160 K at a pressure above 30 GPa [26-28]. Copper oxycarbonates high-temperature superconductors were discovered by Maignan et al. [29], in 1993. Tallon et al. [30], in 1999, discovered the high-temperature ferromagnetic superconductor in $RuSr_2GdCu_2O_8$. The rutheno-cuprate $RuSr_2GdCu_2O_8$ possesses a remarkable property of superconductivity at $T_c \approx 46$ K. Finally, in 2003 intermetallic magnesium compounds superconductor MgB_2 with T_c = 39 K was discovered by Akimitsu et al. [31, 32].

In 1935, Fritz and Heinz London [33] presented equations to describe the Meissner effect and projected the extent to which a magnetic field might permeate a superconductor. Ginzburg and Landau made a significant theoretical breakthrough in 1950 with the GL theory [34], which defined superconductivity and offered a derivation for something like the London equations. Landau's theory on second-order phase transitions was merged with a Schrödinger-like wave equation in this theory, which was very successful in describing the macroscopic features of superconductors. Abrikosov demonstrated that Ginzburg-theory Landau predicts the classification of superconductors into two types, presently known as type I and type II superconductivity. In 2003, Abrikosov and Ginzburg received the Nobel Prize for their work.

2. (Cu, Tl)-1223 phase

High-temperature superconductors (HTSCs) are compounds that have a superconducting transition temperature T_c above 30 K. In 1986, a truly breakthrough discovery was made in the superconductivity field by Bednorz and Müller [35]. They discovered superconductivity in $LaBaCuO_4$, which had a superconducting transition temperature of 35 K. Shortly after, superconductivity with T_c greater than 90 K was discovered in the $YBa_2Cu_3O_{7-\delta}$ compound. This was important because liquid nitrogen could then be used as a refrigerant (at atmospheric

Advanced Carbon Journal, 2024, Vol. 1, Iss. 1, 93-110
DOI: 10.62184/acj.jacj1000202425

Review Article

pressure, the boiling point of nitrogen is 77 K), hence opening the door for more commercial applications. In 1988, $Bi_2Sr_2Ca_2Cu_3O_{10+\delta}$ and $Tl_2Ba_2Ca_2Cu_3O_{10+\delta}$ were discovered with T_c up to 110 K and 125 K, respectively. The highest superconducting transition temperature, at ambient pressure, is recorded for $HgBa_2Ca_2Cu_3O_{8+\delta}$ at 135 K and it was possibly to reach 164 K under high pressure of 31 GPa. Later in 1994, a nontoxic superconductivity was found in $CuBa_2Ca_2Cu_3O_{10-\delta}$, Cu- 1223, superconductor with T_c equal to 120 K prepared under high-pressure synthesis. In 2008, a new class of superconductors named pnictide based on iron and arsenic was discovered [35], with T_c~55 K [36]. Table 1.1 displays the superconducting transition temperature of some high-temperature superconductors (HTSCs) and Iron-based superconductors.

Table 1. Superconducting transition temperatures of some HTSCs and Iron based superconductors.

Material	T_c (K)	Class
$HgBa_2Ca_2Cu_3O_{8+\delta}$	135	High-temperature superconductors
$Tl_2Ba_2Ca_2Cu_3O_{10+\delta}$	125	
$CuBa_2Ca_2Cu_3O_{10-\delta}$	120	
$Bi_2Sr_2Ca_2Cu_3O_{10+\delta}$	94	
$YBa_2Cu_3O_{7-\delta}$	92	
$SmFeAsO_{0.85}$	55	Iron-based superconductors
$CeFeAsO_{0.84}F_{0.16}$	41	
$LaO_{0.89}F_{0.11}FeAs$	26	

Large-scale applications of high-temperature superconductors require superconductors with high J_c (> 1×10^5 A/cm^2) operating at 77 K in a strong magnetic field (10-20 T). Some cup rate HTSCs have sufficiently high T_c values (T_c > 116 K). However, some challenges are faced in large-scale applications such as strong superconducting anisotropy, their irreversible field (Birr= 10 T), and J_c values under high field at 77 K not high enough [35, 36]. High-performance superconductor of Nb_3Al [37] was obtained with J_c value at 77 K comparable to or higher than J_c of 4×10^5 A/cm^2 at 10 T and 4.2 K. For J_c of 1×10^3 A/cm^2 at 77 K. The highest performance of HTSCs has a high irreversible field Birr exceeding 30 T. Both $CuBa_2Ca_{n-1}Cu_nO_{2n+4-\delta}$ [38-40] and $TlBa_2Ca_{n-1}Cu_nO_{2n+3-\delta}$ [41, 42] systems, Cu-12(n-1) n and Tl-12(n-1) n systems had studied and these systems had isostructural to one another.

Cu-12(n-1) n was synthesized at high pressures and temperatures, whereas Tl-12(n-1) n was synthesized at moderate temperatures and pressures [38-44]. The hybrid charged reservoir layer containing Tl and Cu was predicted to preserve the low superconducting anisotropy [45]. Ihara et al. tried similar experiments [46] in thin films and designated this system as (Cu, Tl)- 1223. Therefore, the (Cu, Tl)-1223 phase is considered a moderated phase between Tl1223 and Cu-1223. Consequently $(Cu_{0.5}\ Tl_{0.5})$-1223 system was selected because of the simplest methods of preparation, high T_c, low anisotropy, and the availability for practical applications. $(Cu_{0.5}\ Tl_{0.5})$-1223 is identical to Cu-1223 in the number and the nature of superconducting CuO_2 layers while it differs in their charge-reservoir layers, $Cu_{0.5}\ Tl_{0.5}\ Ba_2O_{4-\delta}$ as shown in Figure 1.3. $Cu_{0.5}Tl_{0.5}\ Ba_2Ca_2Cu_3O_{10-\delta}$, as a superconducting compound, has a P4/mmm space group and tetragonal structure. The unit cell has one $Cu_{0.5}T1_{0.5}\ Ba_2O_{4-\delta}$ charge-reservoir layer and three CuO_2 layers. CuO_2 layers and are separated by two Ca atoms, while charge reservoir layers with CuO_2-planes are separated by two Ba atoms. Central-planes or S-planes are CuO_2 layers separated by Ca atoms. On the other hand, P-planes are planes divided by Ca atoms on one side and $Cu_{0.5}Tl_{0.5}\ Ba_2O_4$ charge-reservoir on the other side. The carriers are over-doped in the P-planes,

Advanced Carbon Journal, 2024, Vol. 1, Iss. 1, 93-110

DOI: 10.62184/acj.jacj1000202425

Review Article

whereas the carriers are optimally doped in the S-planes. P planes also act as a conduit for carriers from the charge reservoir layer to S planes. Cu (2) and O (4) are the names given to the copper and oxygen atoms in the S-planes, respectively. In the P-planes, Cu and O atoms are designated as Cu (1) and O (1), respectively. O (2) atom is the apical oxygen atom that connects the $Cu_{0.5}Tl_{0.5}Ba_2O_4$ charge-reservoir layer to the P-plane. The supply of carriers to the P-planes and their doping from the charge-reservoir layer is virtually controlled by this atom. Finally, the O atom at the core of $Cu_{0.5}Tl_{0.5}Ba_2O_{4-\delta}$ - plane is referred to as the charge reservoir layer's O (3) atom or O (2). It is well known that Tl-1223 has a high critical current density J_c, which makes it a potentially valuable material for the production of superconducting wires, tapes, electric power cables, magnets for maglev trains, electric motors, superconducting quantum interference devices (SQUID), single flux quantum (SFQ) devices and thin-film applications [47]. For example, an important potential application of the new superconducting film process is to fabricate conductors for magnet coils. Such coils are necessary for high-temperature (77 K) superconducting generators and motors to become practical. They also would be useful for magnetic resonance imaging, magnetically levitated trains, microwave power generators, particle accelerators, and any other applications that are useful for the production of high magnetic fields. Since the new films can carry $6x10^5$ A/cm^2 at the temperature of liquid nitrogen, 77K, the current carrying capacity is even higher at lower temperatures. The new films in magnetic fields are the subject of further study, but it is already clear that the properties are rather good. For example, in a magnetic field of 0.4 Tesla, the films can carry 10^6 A/cm^2 at 20 K. These new films can be used in magnets, motors, generators, and superconducting solenoid energy-storage devices; the new thin film process also has potential uses in electronics. For instance, the new thin film process may prove useful in multi-chip modules where many semiconductor chips are to be linked with superconducting interconnects. Moreover, the Tl-1223 superconducting phase has been considered as a prospective material due to various applications such as magnetic shields, resonators, microwave filters, and antennas [37].

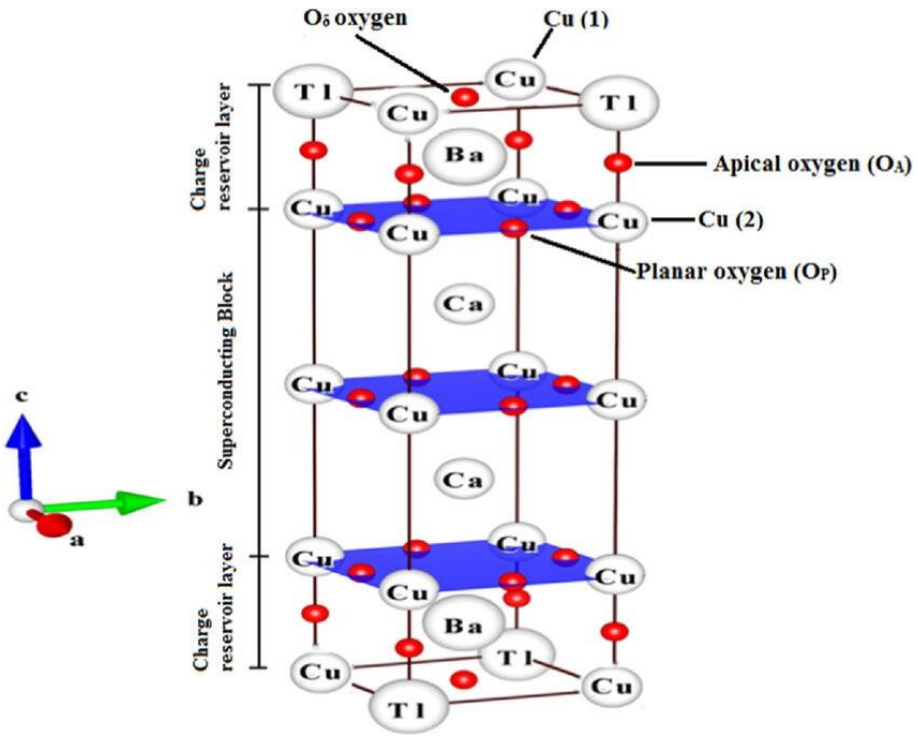

Figure 3. The crystal structure of (Cu 0.5Tl 0.5)-1223.

Advanced Carbon Journal, 2024, Vol. 1, Iss. 1, 93-110
DOI: 10.62184/acj.jacj1000202425

Review Article

3. Nanoparticles in HTSCs

HTSCs have a high critical current density (J_c) in strong magnetic fields for practical applications, particularly power applications. Increasing J_c at higher fields can be accomplished by introducing effective vortex pinning centers. Pinning occurs because of inhomogeneity and microstructure flaws, and it can be boosted by adding artificial pinning centers just in order of the coherence length [48]. Nanosized particles, that introduce strong flux pinning centers to bulk superconductors, are one of the most effective ways to improve J_c [49–55]. Direct magnetic interactions of the vortex and magnetic pinning centers can improve the pinning strengths of flux lines in HTSCs. Strong interaction between the flux line network and the magnetic system can be expected of magnetic particles with characteristic length [56-57]. Different types of nanoparticles can be added to superconductors.

3.1. Carbon nanotubes in superconductors

Yeoh et al. in 2005 studied the carbon nanotubes embedded in the MgB_2 matrix and they found that some of the nanotubes were unreacted and entangled. Magnetization experiments showed that the critical current density changes with nanotube length but not with outer diameter. This suggested that longer nanotubes have a propensity to entangle and inhibit uniform mixing and dispersion with MgB_2. Overall, MgB_2 doped with carbon nanotubes had a higher critical density and a lower critical temperature [58-59]. Anas et al studied the impact of adding single-wall carbon nanotubes (SWCNTs) and multiwall carbon nanotubes (MWCNTs) on the Vickers microhardness of the Gd-123 superconducting phase. Samples of type (SWCNTs)x and (MWCNTs)x$GdBa_2Cu_3O_{7_\delta}$ were generated using the solid-state reaction approach, where 0.0 x 0.1 wt% for samples with SWCNTs and MWCNTs added, respectively. The observed results demonstrated an improvement in phase formation and grain connection up to 0.06 and 0.08 weight percent. Similarly, the superconducting transition temperature T_c increased at low CNT concentrations but decreased at larger ones [60].

Ocicek et al**.** explored the effects of introducing multi-wall carbon nanotubes (MWCNTs) to a $Y1Ba_2Cu_3O_x$ high-temperature superconductor system. The core matrix was expanded with MWCNTs. Investigations were done on the material produced by structural development and electrical transport. The results showed that while the transport critical current density, J_C^{Tran}, increased at least six times more than in pure YBCO samples, the superconducting onset temperature, T_C, did not vary much [61]. Hannachi et al. investigated the production and characterization of bulk $YBa_2Cu_3O_{7-\delta}$ superconductors that were made using the solid-state reaction pathway and varied amounts (x) of CNTs (x = 0.0, 0.1, and 1.0 wt%). The results investigation showed that different sintered samples had successfully achieved the orthorhombic YBCO phase. With CNTs included, no appreciable change in the lattice characteristics was seen, and showed that the CNTs were dispersed throughout the YBCO. Additionally, the critical current density J_c was established, and it was shown that the presence of CNTs in the applied magnetic field significantly increased its value [62].

Elsabawy prepared a composite of 2212-BPSCCO with carbon nanoparticles (HCNs/Pt) as a mechatronic tensile strength promoter. The sample with x = 0.4 mol of HCNs/Pt produced the highest hydraulic tensile strength value of 45.77 MPa, with a promotion ratio of 21.08%, in comparison to the pure-sample x = 0 and mechanical tension of 37,8 Mpa. Additions of hollowed carbon nanoparticles (HCNs/Pt) did not impair superconductivity on the investigated range, even though Tc-values notably decreased and measured $T_{coffset}$= 62.2 K was only for samples with the maximum addition ratio x = 0.4 mol; instead, $T_{coffset}$ = 67.11 K for pure 2212-BPSCCO [63].

3.2. Graphene and Graphene oxide in superconductors

Anas, et al investigated superconductivity specimens of kind $(GO)_x/(Cu_{0.25}Tl_{0.75})$ $Ba_2Ca_3Cu_4O_{12-\delta}$, $0 \leq x \leq 2$ wt%, which prepared at 850 °C under ambient pressure by using a single-step solid-state reaction approach. The predicted

DOI: 10.62184/acj.jacj1000202425

interplanar distance of GO was 0.967 nm, demonstrating the existence of o_2 ligands on the entire surfaces of GO sheets. The T_c of the pure substance $(Cu_{0.25}Tl_{0.75})Ba_2Ca_3Cu_4O_{12-\delta}$ was an acceptable value for the superconducting transition temperature. The inclusion of GO served as just an interface here between superconducting grains but did not alter the host material's crystal structure. The findings from studies revealed that now the sample with x = 0.75 wt% had an exceptional maximum enhancement in phase formation, grain connectivity, and T_o [64]. Sudesh et al. studied the effects of simultaneous addition of GO and citric acid on the superconducting characteristics of MgB_2 by synthesizing polycrystalline samples with compositions of MgB_2 + 3wt% GO + x wt% $C_6H_8O_7$ (x = 0, 5 and 10). All generated samples exhibited the hexagonal MgB_2 crystal structure with space group P6/mm, according to X-ray diffraction measurements. The findings demonstrated that the addition of GO to the sample improves grain connection, which then greatly increases the critical current density without significantly altering T_c. Hc_2 and Hirr, however, have not significantly improved for this sample. When GO and citric acid are added together, the $J_C(H)$, Hc_2, and Hirr were seen to significantly improve in comparison to the pristine MgB_2 and GO-supplemented MgB_2 samples. When compared to a sample of pure MgB_2, for instance, the J_C (10 K, 5 T) of sample x = 10 had improved by a factor of~5, and when compared to sample x = 0, it had improved by a factor of ~5.5. Additionally, $Hc_2(0)$ for the sample at x = 10 had grown by 13 T when compared to pure MgB_2, whereas it had increased by 10 T when compared to the sample at x = 0. The combination of GO and citric acid together had led to the observation of improved flux pinning [65].

The effect of graphene on the transport critical current density of $(Tl_{0.85}\ Cr_{0.15})\ Sr_2CaCu_2O_{7-\delta}$ (Tl-1212) superconductor was examined by Kong et al. The properties of the samples were determined using solid-state reaction technology and high-purity oxide powders. It was found that the zero-resistance, or T_C-Zero, decreased from 95 K to 84 K with the addition of additional graphene. The transport critical current density (J_c) of pure and graphene-added bulk samples was studied with temperature. At 30 K, the bulk sample's J_c was 1320 mA/cm^2, but the sample containing 0.001 weight percent of graphene had a J_c of 3660 mA/cm^2. The results showed that with increasing graphene addition, the J_c of the Tl-1212 samples decreased. As an impurity, graphene is thought to have performed the flux pinning effect on Tl-1212. J_c rose in Tl-1212 superconductors as a result [66]. Bibekananda Sahoo and colleagues reported on the structural modification and superconducting parameter variation of $YBa_2Cu_3O_{7-\delta}$ (YBCO) high-temperature superconductor (HTSC) with the addition of various weight percentages of graphene nano-platelets (GnPs) (0.0, 0.5, 1.0, 2.0, & 3.0 wt.%) synthesized via standard solid-state reaction route. All of the samples with the P_{mmm} space group had orthorhombic structures, which were confirmed by the XRD analysis by Rietveld refinements. The orthorhombic YBCO superconducting matrix's lattice properties did not noticeably alter when GnPs' weight percentage increased. The field emission scanning electron microscopy analysis of the GnPs doped samples revealed a better connectivity between the grains. There was no chemical reaction between superconductivity and GnPs, as shown by the fact that the addition of GnPs decreased the room temperature resistivity and—more importantly—increased the critical temperature. The critical current density value for TBCO samples with GnPs substitutions had actually risen. When 0.4 T external magnetic fields were applied, the critical current density for a 2.0-weight percent GnPs doped sample was at its maximum and approximately 12 times more than that of pure YBCO [67].

3.3. Metal nanoparticles in superconductors

Mohammed et al. successfully manufactured (nano-Ag)$xCu_{0.5}\ Tl_{0.5}\ Ba_2Ca_2Cu_3O_{10-\delta}$, $0.0 \leq x \leq 3.0$ wt% ceramic superconducting samples using a single-step solid-state reaction method at 850 ^oC and ambient pressure. The sample with x = 0.15 wt% had the highest volume fraction of grains connected, according to the data obtained. The electrical resistivity measurements were used to investigate the prepared samples'

DOI: 10.62184/acj.jacj1000202425

electrical characteristics, and the findings demonstrated that the maximum superconducting transition temperature (T_c) was found at x = 0.15 weight percent. For all samples, excess conductivity measurement revealed a transition from two dimensions (2D) to three dimensions (3D) when the temperature dropped [68]. To create (Ag)x/CuTl-1223 composites, Khan et al. in 2020 introduced Ag nanoparticles to CuTl-1223 host superconductor at x = 1, 2, 3, and 4 wt% concentrations. The crystal symmetry of the CuTl-1223 phase was unaffected by the addition of nanoparticles, according to XRD results, which suggested that the nanoparticles were deposited at the grain boundaries [69]. Abdeen et al. investigated the effects of nanosized Ag addition to phase development as well as the electrical properties of the superconducting phase ($Cu_{0.5}Tl_{0.25}$)-1223. They discovered that a small amount of nanosized Ag (x=1.5 wt%) increased phase formation and improved T_c, J_c, and melting temperature. A reversal trend was seen for x >1.5 wt. Percent [70].

The effects of introducing metallic Cu nanoparticles only on the development of the polycrystalline $Cu_{0.5}$ $Tl_{0.5}$ $Ba_2Ca_2Cu_3O_{10-\delta}$ (CuTl-1223) superconducting phase were examined by Liaqat Ali et al. The results after the addition of Cu nanoparticles, the crystal structure of the host CuTl-1223 phase did not change (remaining tetragonal), which provided information regarding the occupancy of these nanoparticles at the inter-crystallite sites. These metallic Cu nanoparticles were thought to be the greatest candidate for enhancing intergrain connectivity and superconducting characteristics, and their inclusion increased grain shape and intergrain connectivity. The CuTl1223 phase was found to predominate, along with a few other superconducting phases and unknown impurities, according to the calculation of the superconducting volume fraction. The CuTl1223 phase's ideal concentration of Cu nanoparticles for maximizing the improvement of superconducting characteristics was 1.0 wt% [71].

Rahima et al. examined the $(M)_z$/CuTl-1223; (M = Co or Cr) nanoparticle/superconductor composites' dielectric response in 2020. Solid-state reactions were used to prepare the CuTl-1223 superconducting phase. Various samples were created with the correct NP ratios (x=0, 0.5, 1, and 1.5 wt%). According to XRD, the host material's crystal structure didn't change, which suggested that the NPs had settled down at the inter grain locations. Co and Cr NPs addition lowers the superconductor's critical temperature (T_c). The greatest values of the dielectric constants ε'(ω), ε"(ω), and tanδ were found at lower frequencies, becoming saturated at higher frequencies, whereas the ac conductivity σ_{ac} grows linearly up to 5×10^6 Hz and then sharply after that. In the case of Cr NPs compared to Co NPs. ε'(ω) was less suppressed while ε"(ω) and tanδ were boosted more [72].

3.4. Metal oxide nanoparticles in superconductors

Khulud Habanjar et al. investigated the microstructure, phase development, and mechanical properties of the (Bi,Pb)-2223 superconducting phase in 2019. Solid-state reactions and co-precipitation were used to produce $BaFe_{12}O_{19}$ nanoparticles and $(BaFe_{12}O_{19})$x(Bi,Pb)-2223 superconducting samples, respectively. $BaFe_{12}O_{19}$ nanoparticles and $(BaFe_{12}O_{19})$x(Bi,Pb)-2223 structures were studied using X-ray diffraction, and the experimental results revealed that the Bi-2223 phase contains traces of the Bi-2212 secondary phase. $BaFe_{12}O_{19}$ addition had little effect on the lattice parameters, indicating that nanoparticles do not enter the host crystal of (Bi,Pb)-2223. Vickers microhardness H_v was calculated as a function of the time and indentation force. It was discovered that the relationship between microhardness and applied stress and time is nonlinear. Various models were used to assess the experimental results. The investigation showed that the HK model was more effective at calculating the load than the other methods [73].

Rekaby looked into how the superconducting and dielectric properties of $Cu_{0.5}$ $Tl_{0.5}$ $Ba_2Ca_2Cu_3O_{10-\delta}$, CuTl-1223, affected by the addition of $Zn_{0.91}$ $Mn_{0.03}$ $Co_{0.06}O$ NPs in 2020. $Zn_{0.91}$ $Mn_{0.03}$ $Co_{0.06}O$ NPs were prepared using the wet chemical co-precipitation technique. By using the common solid-state reaction method, four samples of type $(Zn_{0.91}$ $Mn_{0.03}$ $Co_{0.06}O)x$ /

DOI: 10.62184/acj.jacj1000202425

CuTl-1223, with x = 0.00, 0.02, 0.06 and 0.10 wt.%, the result showed the samples have a single CuTl-1223 phase with a tetragonal structure and the addition of $Zn_{0.91}Mn_{0.03}Co_{0.06}O$ did not change the phase's structure. After the addition of $Zn_{0.91}Mn_{0.03}Co_{0.06}O$, SEM micrographs of the CuTl-1223 samples appeared to reveal a suppression of voids. Additionally, the addition of NPs reduced the samples' randomly oriented plate-like shape and transformed it into well-connected spherical grains. The superconducting transition temperature (T_c) of the CuTl-1223 phase increased to 124.5 K by the addition of $Zn_{0.91}Mn_{0.03}Co_{0.06}O$ NPs in minor concentration (x = 0.02 wt%), and the findings showed that all of the dielectric properties substantially depended on frequency as well as the addition of NPs, and that the samples had enormous dielectric constants with little dissipation in the low-frequency range [74]

$Cu_{0.5}Tl_{0.5}Ba_2Ca_2Cu_3O_{10-\delta}$, $(Cu_{0.5}Tl_{0.5})$-1223, combined with nano-Fe_2O_3 (0.0-1.0 wt.%) was created using a solid-state reaction approach via short time preparation procedure and under ambient pressure in a study by Aly Abou-Aly et al. in 2020. The volume fraction data showed that, particularly for samples with x 0.2 wt.%, adding nano-Fe_2O_3 significantly increased the pace at which the $(Cu_{0.5}Tl_{0.5})$-1223 phase formed. T_c was observed up to x = 0.2 wt% before systematically declining as the amount of nano-Fe_2O_3 increased, and the findings made it clear that all of the dielectric characteristics exhibited a significant temperature dependence at low and intermediate frequency ranges. Additionally, they were highly reliant on the presence of nano-Fe_2O_3, whose high content (x = 1.0 wt%) increased ε' and decreased tanδ of the $(Cu_{0.5}Tl_{0.5})$-1223phase [75].

Albiss et al. looked at the impact of adding nanosized NiO just on polycrystalline (Bi, Pb)-2223 phase development and flux pinning. The results showed that when the volume fraction of the high T_c phase (2223) was reduced to higher nanosized NiO adding, the volume percentage of the low T_c phase (2223) increased (2212). However, for all samples, there was essentially little change in T_c. Nanoparticle addition suppressed vortex pinning forces at all concentrations by x higher than or equal to 0.005 throughout all temperatures [76].

In 2022, Baqi et al studied the effects of MgO NPs with a particle size average of less than 100 nm to the Bi2223 superconductivity systems. The bulk samples were created using the conventional solid-state and had a nominal composition of $Bi_{1.6}Ag_{0.4}Sr_{1.9}Ba_{0.1}Ca_2Cu_3O_{10+\delta} + (MgO)_x$ (x = 0,0.1, 0.2, and 0.3 wt%). The results revealed that the addition of more nano Mg changes the lattice parameters and increases the volume fraction of the Bi2223 phase. In contrast to additional samples with micro MgO, the specimen with adding 0.3wt% MgO exhibited the highest Bi2223 phase volume (about 80%) and highest superconduction temperature gradient, T_c (up to 141K) [77].

Wan et al. [78] investigated the influence on nanosized MgO in (Bi, Pb)-2223silver-sheathed J_c of samples containing nanosized MgO is found to be 1.2 times higher than that of samples containing no MgO in zero applied electrical field and 1.4 times higher in a magnetic field range from 0.1 to 1 T at 77 K. Nasri and his colleagues. [79] investigated the effect of adding nanosized MgO particles to the Bi–2212 superconducting phase's superconducting and mechanical properties. The addition of 5% nano-size MgO particles provided the highest J_c. Awad [80] investigated the effects of nanosized MgO injection on the $(Cu_{0.25}Tl_{0.75})$-1234 phase's phase evolution, microstructure, electrical properties, and mechanical properties. By including nanosized MgO up to 0.6 wt%, phase formation, grain connectivity, transport critical current density, and microhardness were improved. While the increase in J_c was linked to the pinning effect on nanosized MgO, the rise in microhardness was attributed to an increase in grain connectivity and crack resistance propagation. However, increasing the amount of nanosized MgO > 0.6 wt.% decreased microhardness, grain connectivity, and microphase formation. It was believed that this was caused by a significant amount of nanosized MgO aggregating between the grains, which decreased the

DOI: 10.62184/acj.jacj1000202425

superconducting grain connection and worsened the intergranular critical current density.

Jia et al [81] studied the effect of adding nanosized ZrO_2 to the bulk (Bi,Pb)-2223 flux pinning capability. They discovered that nano-ZrO_2 particles have no discernible influence on T_c. However, studies of J_c revealed that adding a small amount of nanosized ZrO_2 dramatically increased J_c values with applied magnetic fields. By mixing nanosized ZrO_2 with precursor before melt development in air, Xu et al. [50] successfully inserted nanosized centers for magnetic flux pinning into a bulk superconductor $GdBa_2Cu_3O_7$. The results showed that during the melt process, nanosized ZrO_2 interacted with Gd-123 to create $BaZrO_3$ particles with a size of roughly 50 nm. For x=0.004 mol percent, the J_c value was increased to 100,000 A/cm^2 at 77 K with self-field.

Xu et al. [51] studied the effects of nanosized SnO_2 and ZrO_2 powders on the Gd-123 system. The results showed that nanosized SnO_2/ZrO_2 addition had no effect on the T_c of Gd-123 bulk, but that the J_c value increased from 62,900 to 99,300 & 80,400 A /cm^2 at 77 K with self-field for such sample 0.004 mol percent ZrO_2 and 0.008 mol percent SnO_2, respectively. The top seeding melt growth approach was used to successfully manufacture Gd-123 bulk, with nanosized (ZrO_2 + SnO_2 + ZnO) spanning between 0 to 0.006 mol percent as a second phase into the Gd-123 matrix [58]. The samples with 0.006 mol percent nanosized (ZrO_2 + SnO_2 + ZnO) showed an increase in the trapped field and J_c values. The greatest J_c of the bulk was found to be 72,500 A/cm^2 at 77 K also with the self-field. Nanosized particle inclusions in Gd-123 matrices were found to produce pinning centers, which increased the J_c of the samples.

Annabi et al. [82] inserted nanosized Al_2O_3 into (Bi, Pb)-2223 precursor powders during the final sintered cycle of a multi-step preparation process. The impact of nanosized Al_2O_3 on the melting temperature, phase formation, microstructure, and transport characteristics of (Bi, Pb)-2223 was investigated. They found that adding a small quantity of Al_2O_3 (0.2 wt%) to the sample raised Jc by 30% at 77 K and improved J_c behavior in magnetic fields parallel or orthogonal to the sample broad surface. Sengupta et al. [83] investigated melt-processed Tl-1223 phase pellets with or without nanosized Al_2O_3 injection. Nanosized Al_2O_3 additions seemed to not affect T_c, according to the researchers. J_c increased considerably for all samples with nanosized Al_2O_3 additions at temperatures below 35 K. The nanosized Al_2O_3 modifications had only a minor influence on Jc at 77 K. High concentrations of defects just on the order of nanosized additions are effective at pinning flux lines analytically.

Abou-Aly and his colleagues. [84] looked examined how varied concentrations of nanosized SnO_2 (x = 0.0 to 2.0 wt%) affected phase formation, microstructure, electrical, and thermal properties of the (Bi, Pb)-2223 phase. They discovered that increasing the volume Percent, T_c, and J_c by adding nanosized SnO_2 up to x = 0.4 wt% boosted the volume fraction, T_c, and J_c. A pinning effect on nanosized SnO_2 was thought to be responsible for the increase in Jc. The phase formation, T_c, and J_c of the (Bi,Pb)-2223 phase were lowered at greater concentrations of nanosized SnO_2 x > 0.4 wt. percent. The high concentration of nanosized SnO_2 caused significant agglomerations between superconducting grains, resulting in diminished superconducting grain connection and worsened intergranular critical current density.

Elokr et al. [85] used the co-precipitation approach and a one-step solid-state process to make nanosized ZnO and $(Cu_{0.5}Tl_{0.25}Pb_{0.25})$-1223 superconducting phase, respectively. The addition of nanosized ZnO up to 0.8 wt% improved the volume percentage of the $(Cu_{0.5}Tl_{0.25}Pb_{0.25})$-1223 phase and improved both T_c and J_c. This phase's melting point increased from 879 °C, x = 0 to 893 °C, x = 0.4 wt.%. The volume fraction, T_c, J_c, & melting point $(Cu_{0.5}Tl_{0.25}Pb_{0.25})$-1223 phase were lowered as x increased (x > 0.8 wt%).

The influence of nanosized ZrO_2 and ZnO inclusions on the superconductive characteristics of the melt-processed $GdBa_2Cu_3O_{7-\delta}$ -bulk superconductor was investigated by Xu et al. [49]. The experimental results revealed that a small amount

DOI: 10.62184/acj.jacj1000202425

of nanoparticles ZrO_2 and ZnO (x=0.004 mol percent) added to the Gd-123 bulk superconductors improved the J_c and irreversibility field Birr.

$(Cu_{0.5}Tl_{0.25})$-1223 superconducting phase's phase formation, microstructure, electrical, and mechanical properties were studied by Mohammed et al. with the effects of nanosized SnO_2 [86], In_2O_3 [87], and Fe_2O_3 [88]. The results showed that adding nano-SnO_2 increased both the volume percentage and T_c up to x = 0.6 wt% and the microhardness up to x = 1 wt%. T_c increased somewhat with x, whereas the addition of nano-In_2O_3 nearly had no effect on the percentage of the phase over all values of x. Up to x = 0.1 wt%, the quantity of nanosized In_2O_3 added enhanced the microhardness; after that, it decreased as the amount of nanosized In_2O_3 increased. By adding nanosized Fe_2O_3 above x=0.2 wt%, the volume percent and T_c were improved. On the other hand, as the amount of nanosized Fe_2O_3 added rose up to x = 1 wt%, microhardness increased.

Matar and others in 2022 discovered that the microhardness values of (Bi, Pb)-2212 modified with nano-CdO, nano-CdMnO, & nano-CdFeO steadily increased up to x= 0.05 wt%, demonstrating the improvement of the grain-to-grain connections. In contrast to the pure samples and its two additions, CdO and CdMn, CdFeO addition surpassed CdO and CdMnO adding in enhancing HV inside the plateau area, with improvements of 113.83%, 20.44%, and 4.75%, respectively [89].

3.5. Bi_2Te_3 and $BaCO_3$ nanoparticles in superconductors

The impact of Bi_2Te_3 nanoparticles on the structural and physical characteristics of Bi-2223 was examined by Shalaby et al. in 2021 for the polycrystalline "$(Bi_{1.6}Pb_{0.4}Sr_2Ca_2Cu_3O_{10+\delta})_{1-x}/(Bi_2Te_3)_x$" where "(x = 0.00,0.01,0.02 & 0.03)". The obtained results had generated two intriguing hypotheses regarding the interaction of Bi_2Te_3 nanoparticles with both the granular BSCCO superconductivity network. First, when the amount of Bi_2Te_3 nanoparticles grew, the volume percentage of the Bi-2223 phase, as well as the Bi-2212 phase marginally shifted toward one another. In comparison to samples without the addition of Bi_2Te_3 nanoparticles, additional samples significantly affected the lattice constants and other microstructure characteristics. Due to the presence of Bi_2Te_3 nanoparticles, the starting temperature of BSCCO phases were not significantly impacted; nevertheless, the slower diamagnetic transitioning was recorded for (Bi_2Te_3 with x = 0.01). Second, when comparing to the other samples, the pure sample exhibited the greatest Jc values—1.5* 104 & 350 A/cm^2 at 5 & 50 K, respectively—as well as Hirr, Hmax, and Fp-max. These findings demonstrated the influence of Bi_2Te_3 nanoparticles on magnetic and superconducting properties. Bi_2Te_3 nanoparticles were thought to have an impact on flux pinning, hysteresis loop lengths, and critical current densities despite the material's non-magnetic nature [90].

A. Akbar1, et al. in 2021 found a great impact on the critical temperature (T_c) for the Bi-Pb-Sr-Ca-Cu-O superconductor by adding a small amount of $BaCO_3$. A greater critical temperature was achieved by adding 1%wt $BaCO_3$ as opposed to 2%wt $BaCO_3$. The critical temperature (T_c) dropped as the amount of $BaCO_3$ increased. Tconset = 86 K and Tczero = 52 K were the ideal critical temperatures (T_c) that were generated. At a temperature of 86 K and higher, the sample exhibited the existence of semiconductor characteristics. Phase (Bi-Pb) -2212 was the major phase in this sample, although there was also a small number of phases (Bi, Pb) -2223 in terms of volume percent [91].

4. Conclusion

In this review, according to XRD, $(Cu_{0.5}Tl_{0.5})$-1223 kept its tetragonal structure even after the addition of QDs. The volume fraction data showed that the addition of quantum dots significantly increased the rate at which the $(Cu_{0.5}Tl_{0.5})$-1223 phase formed. SEM micrographs showed that the pure sample's morphology consisted primarily of irregularly shaped and spherical grains interspersed among randomly oriented plate-like grains. The inclusion of the quantum dots raised the density of the microstructure and decreased the porosity between the

DOI: 10.62184/acj.jacj1000202425

grains. The electrical resistivity's temperature dependency of the samples displayed a transition to the superconducting state below Tc and metallic behavior above Tc. For respect to $(QD)_xCu_{0.5}$ $Tl_{0.5}$ $Ba_2Ca_2Cu_3O_{10-\delta}$, the electrical resistivity experiments showed that Tc increased. For $(QD)_xCu_{0.5}$ $Tl_{0.5}$ $Ba_2Ca_2Cu_3O_{10-\delta}$ the critical current density Jc and flux pinning energy U rose. Vickers microhardness studies revealed that Hv rapidly declined up to 1.96 N of applied load before exhibiting a load-independent plateau at applied force > 1.96 N., the microhardness values rose with the addition of with different QDs. Improvements in the $(Cu_{0.5}Tl_{0.5})$-1223 phase's microhardness were attributed to the reduction of porosity, the grains' resistance to crack propagation, and the increased grain connectivity on by the addition of quantum dots.

Authors Information

Corresponding Author: Batool Jabbar Obaid AL Toofan*

E-mail: batool.j@uokerbala.edu.iq

References

[1] Kopnin, N. B. (2009). Introduction to the Theory of Superconductivity. Helsinki University of Technology, P 5,.

[2] Abdul Rahman, M. W. (2019). Preparation of superconducting Y-Ba-Cu-O compounds and study their structural and electrical properties. University of Baghdad College of Education for Pure Science Ibn-ALHaitham.

[3] Subedi, M.S. (2017). Superconductivity and Cooper Pairs. Himalayan Physics, 6 and 7, 107. https://doi.org/10.3126/hj.v6i0.18371

[4] Saxena, A. K.(2012). High-Temperature Superconductors. 2nd Edition. Springer, https://doi.org/10.1007/978-3-642-28481-6

[5] Mahdi, S. H. Mohammed, L. A. Fadhil, R. N. and Hussein, B. H. (2023). Fabrication and study of characteristics of $HgSr_2$ $Ca_{n-1}Cu_nO_{\delta+10}$, (n = 1, 2 and 3) thin films superconducting. Digest J. Nanomater. Biostruct., 2, 590. https://doi.org/10.15251/djnb.2023.182.579

[6] Tanaka, S. (2001). High-temperature superconductivity: History and outlook. JSAP International, 4.

[7] Korhonen, P., & Voutilainen, R. (2006). Finding the most preferred alliance structure between banks and insurance companies. European Journal of Operational Research, 175, 1285. https://doi.org/10.1016/j.ejor.2005.04.046

[8] Bednorz G. and Müller, K. A. (1986). Possible high Tc superconductivity in the Ba−La−Cu−O system. Phys. Condens. Matter, 64, 189. https://doi.org/10.1007/BF01303701

[9] Sleight, A. W. Gillson, J. L. and Bierstedt, F. E. (1975). Hightemperature superconductivity in the $BaPb_{1-x}Bi_xO_3$ systems, Solid State Commun., 17, 27. https://doi.org/10.1016/0038-1098(75)90327-0

[10] Takagi, H. Uchida, S. Kitazawa K. and Tanaka, S. Japan, J. (1987). High Tc Superconductivity of La-Ba-Cu Oxides. Appl, Phys., 26, L123. https://doi.org/10.1143/JJAP.26.L1

[11] Sinha, M. M. Ashdhir, P. Gupta, H. C. Tripathi, B. B.(1995). Lattice Dynamics of Superionic Cerium Dioxide. PSSb, 191,1. https://doi.org/10.1002/pssb.2221910110

[12] Skakle, J. M. S. Lachowski, E. E. Smith, R. I. and West, A. R. (1997). High-pressure oxidation of the tetragonal $La_{1.5-x}Ba_{1.5+x-y}Ca_yCu_3O_z$ superconductors. Phys. Rev. B, 55, 15228. https://doi.org/10.1103/PhysRevB.55.15228

[13] Yang, Y. F. Wu, D. S. Kao, H. C. I. Wang, C. M. and Wu, M. K. (1995). Superconductivity in the triple-perovskite La-Ca-Ba-Cu-O system. Supercond. Sci. Technol., 8, 874. https://doi.org/10.1088/0953-2048/8/12/004

[14] Peng, J. L. Klavins, P. and Shelton, R. N. (1989). Upper critical field and normal-state properties of single-phase $Y_{1-x}Pr_xBa_2Cu_3O_{7-\gamma}$ compounds. Phys. Rev. B, 39, 9074. https://doi.org/10.1103/PhysRevB.40.4517.

[15] Gunasekaran, R. A. Yakhmi, J. V. and Iyer, R. M. (1993). Synthesis and superconducting properties of

DOI: 10.62184/acj.jacj1000202425

$Ca_{1-x}R_xBaLaCu_3O_{7-\delta}$ (R = CeandNd) systems. Physica C, 208, 143. https://doi.org/10.1016/0921-4534(93)90651-6

[16] Awana, V. P. S. de Lima, O. F. Malik, S. K. Yelon, W. B. and Narlikar, A. V. (1999). Structural and superconducting properties of $LaBaCaCu_3O_{7+\delta}$ system: a neutron diffraction study. Physica C, 314, 93. https://doi.org/10.1016/S0921-4534(99)00035-0

[17] Song, Y. F. Chang, C. N. Kao, H. C. I. Hsieh, C. H. Liu, H. F. Lin, H. D. and Huang, W. W. (1999). O− 1 s x-ray near-edge absorption spectroscopy studies of $La_{1.5-x}Ca_xBa_{1.5}Cu_3O_y$ and $La_{1.5}Ca_xBa_{1.5-x}Cu_3O_y$. Phys. Rev. B, 60, 4357. https://doi.org/10.1103/PhysRevB.60.4357

[18] Wu, M. K. Ashburn, J. R. Torng, C. J. Hor, P. H. Meng, R. L. Gao, L. Huang, Z. J. Wang, Y. Q.and Chu C. W. (1987). Superconductivity at 93 K in a new mixed-phase Y-Ba-Cu-O compound system at ambient pressure. Phys. Rev. Leet., 58,908. https://doi.org/10.1103/PhysRevLett.58.908

[19] Iyo, A. Tanaka, Y. Ishiura, Y. Tokumoto, M. Tokiwa, K. Watanabe T. and Ihara, H. (2001). Study on enhancement of Tc (⩾130 K) in $TlBa_2Ca_2Cu_3O_y$ superconductors. Supercond. Sci. Technol. https://doi.org/14, 504. 10.1088/0953-2048/14/7/313.

[20] Ihara, H. Sugise, R. Shimomura, T. Hirabayashi, M. Terada, N. Jo, M. Hayashi, K. Tokumoto, M. Murata K. and Ohashi, S. (1989). New Tl-Ba-Ca-Cu-O (1234, 1245 and 2234) Superconductors with Very High Tc. Advances in Superconductivity (Proc.1st Int. Symp. on superconductivity, I SS, 88), 1, 793. https://doi.org/10.1007/978-4-431-68084-0_133

[21] Parkin, S. S. P. Lee, V.Y. Engler, E. M. Nazzal, A. I. Huang, T. C. Gorman, G. Savoy, R. and Beyers, R. (1988). Bulk Superconductivity at 125 K in $Tl_2Ca_2Ba_2Cu_3O_x$. Phys. Rev. Lett., 60, 2539. https://doi.org/10.1103/PhysRevLett.60.2539

[22] Parkin, S. S. P. Lee, V. Y. Engler, E. M. Nazzal, A. I. Savoy, R. Beyers, R. and Laplaca, S. J. (1988). $Tl_1Ca_{n-1}Ba_2Cu_nO2_{n+3}$ (n= 1, 2, 3): A new class of crystal structures exhibiting volume superconductivity at up to 110 K. Phys, Rev. Lett.,61, 750. https://doi.org/10.1103/PhysRevLett.61.750

[23] Ihara, H. Sugise, R. Hirabayashi, M. Terada, N. Jo, M. Hayashi, K. Negishi, A. Tokumoto, M. Kimura, Y. and Shimomura, T. (1988). A new high-T_c $TlBa_2Ca_3Cu_4O_{11}$ superconductor with Tc >120K. Nature, 334, 510. https://doi.org/10.1038/334510a0

[24] Maeda, H. Tanaka, Y. Fukutomi, M.and Asano. (1988). A New High-Tc Oxide Superconductor without a Rare Earth Element. Jpn. J. Appl. Phys., 27, L209. https://doi.org/10.1143/JJAP.27.L209

[25] Takada, J. Kitaguchi, H. Egi, T. Oda, K. Miura, Y. Mazaki, H. Ikeda, Y. Hiroi, Z. Takano, M. and Tomii, Y. (1990). Superconductor with Tc = 117 K in the Bi-Pb-Sr-Ca-Cu-O system. Physica C Supercond., 170, 249. https://doi.org/10.1016/0921-4534(90)90319-A

[26] Poole, C. P. (2000). HandBook of superconductivity, Academic press.

[27] Gao, L. Xue, Y.Y. Chen, F. Xiong, Q. Meng, R. L. Ramirez, D. Chu, C. W. Eggert, J. H.and Mao, H. K. (1994). Superconductivity up to 164 K in $HgBa_2Ca_{m-1}Cu_mO_{2m+2+\delta}$ (m= 1, 2, and 3) under quasihydrostatic pressures. Phys. Rev. B, 50, 4260. https://doi.org/10.1103/PhysRevB.50.4260

[28] Awad, R. Costa, G. A. Fenu, M. Ferdeghini, C. El-Sayed, A. H. Abou-Aly, A. I. and Elwahidy, E. F. (1997). Stabilization of mercury cuprates by thallium, superconductivity in $Hg_{1-x}Tl_xBa_2Ca_{n-1}Cu_nO_{2n+2+d}$. IL NUOVO CIMENTO, No 8, 9, 19, 1103. https://doi.org/10.1007/BF03185397

[29] Martin, C. Maignan, A. Huvé, M. Michel, C. Hervieu, M. Raveau, and Eur, J. (1993). The influence of alkaline-earth ions on the properties of the'2201'superconductive cuprates: the solid solution $Tl_2Ba_{2-x}Sr_xCuO_{6\pm\delta}$. Eur. J.Solid State Inorg.Chem., 30, 7.

[30] Bernhard, C. Tallon, J. L. Niedermayer, Ch. Blasius, Th. Golnik, A. Brücher, E. Kremer, R. K. Noakes, D. R. Stronack, C. E. and Asnaldo, E. J. (1999). oexistence of ferromagnetism and superconductivity in the hybrid ruthenate-cuprate compound $RuSr_2GdCu_2O_8$ studied by muon spin rotation and dc magnetization. Phys. Rev B, 59, 14099. https://doi.org/10.1103/PhysRevB.59.14099

[31] Haddon, R. C. Hebard. A. F. Rosseinsky, M. J. Murphy, D. W. Duclos, S. J. Lyons, K. B. Miller, B. Rosamilia, J. M. Fleming, R. M. Kortan, A. R. Glarum, S. H. Makhija, A. V. Muller, A. J. Eick, R. H. Zahurak, S. M. Tycko, R. Dabbagh G. and Thiel F. A. (1991). Conducting films of C60 and C70 by alkali-metal doping. Nature, 350, 320. https://doi.org/10.1038/350320a0

[32] Nagamatsu, J. Nakagawa, N. Muranaka, T. Zenitani, Y. Akimitsu, J. (2001). Superconductivity at 39 K in magnesium diboride. Nature, 410, 63. https://doi.org/10.1038/35065039

[33] London, F. and London, H. (1935). The electromagnetic equations of the supraconductor. Roy. Soc. A149, 71. https://doi.org/10.1098/rspa.1935.0048

[34] Ginzburg, V. L., & Landau, L. D. (1950). Zh. Eksp. Teor. Fiz. Zh. Eksp. Teor. Fiz, 20, 1064.

[35] Blatter, G. Feigel'man, M. V. Geshkenbein, V. B. Larkin, A. I. and Vinokur V. M. (1994). Vortices in high-temperature superconductors. Rev. Mod. Phys., 66, 1125. https://doi.org/10.1103/RevModPhys.66.1125

[36] Cooper, S. L. Gray, K. E. (World Scientific, Singapore1994). Physical Properties of High Temperature Superconductors IV ,61. https://doi.org/10.1142/2244.

[37] Takeuchi, T. Iijima; Y. Inoue; K. Wada, H. (1997). Effect of flat-roll forming on critical current density characteristics and microstructure of Nb/sub 3/Al multifilamentary conductors. IEEE Trans. Appl. Supercond, 7, 1529. https://doi.org/10.1109/77.620864

[38] Mosquera Polo, A. S., Da Silva, R. M., Vagov, A., Shanenko, A. A., Deluque Toro, C. E., & Aguiar, J. A. (2017). Nonequilibrium interband phase textures induced by vortex splitting in two-band superconductors. Physical Review B, 96, 054517. https://doi.org/10.1103/PhysRevB.96.054517

[39] Ihara, H. Yamafuji, K. Morishita, T. (1995). Advances in Superconductivity VII, Springer-Verlag, Tokyo, 225.

[40] Agarwal, S.K. Tokiwa, A. Iyo, K. Tanaka, Y. Tanaka, K. Tokumoto, M. Terada, N. Saya, T. Umeda, M. Ihara, H. Hamao, M. Watanabe, T. and Narlikar, A.V. (1998). Superconductivity in the Mg-doped $CuBa_2Ca_3Cu_4O_{12-y}$ system. Phys. Rev. B 58 ,9504. https://doi.org/10.1103/PhysRevB.58.9504

[41] Ihara, H. Sugise, R. Hirabayashi, M. Terada, N. Jo, M. Hayashi, K. Negishi, A. Tokumoto, M. Kimura, Y. and Shimomura T. (1988). A new High-Tc $TlBa_2Ca_3Cu_4O_{11}$ superconductor with Tc >120K. Nature, 334 ,510. https://doi.org/10.1038/334510a0

[42] Parkin, S.S.P. Lee, V.Y. Nazzal, A.I. Savoy, R. Beyers, R. La Placa, S. J. (1988). $Tl_1Ca_{n-1}Ba_2Cu_nO_{2n+3}$ (n= 1, 2, 3): A New Class of Crystal Structures Exhibiting Volume Superconductivity at up to≃ 110 K. Phys. Rev. Lett. 61, 750. https://doi.org/10.1103/PhysRevLett.61.750

[43] Ihara, H. Tokiwa, K. Tanaka, K. Tsukamoto, T. Watanabe, T. Yamamoto, H. Iyo, A. Tokumoto, M. and Umeda, M. (1997). $Cu_{1-x}Tl_xBa_2Ca_3Cu_4O_{12-y}$ ($Cu_{1-x}Tl_x$-1234) superconductor with Tc=126 K. Physica C Supercond., 282-287, 957. https://doi.org/10.1016/S0921-4534(97)00592-3

[44] Yamamoto, H. Tanaka, K. Tokiwa, K. Hirabayashi, K. Tokumoto, M. Khan, N.A.and Ihara, H. (1998). Synthesis of $Cu_{1-x}Tl_xBa_2Ca_2Cu_3O_{11-y}$ (x∼0.7) superconductor by hot press. Physica C Supercond., 302, 137. https://doi.org/10.1016/S0921-4534(98)00192-0

[45] Alam, S. Oyanagi, H. Mohamed, S. B. Ihara, H. Iyo, A. Kito, H. Badica, P. Rahman M. O. and Yanagisawa. T.

(2001). EXAFS study of $Tl_{0.75}Cu.25BaCa_3Cu_4O_y$ and $Cu_{0.68}C_{.32}Ba_2Ca_3Cu_4O_y$ superconductors [bulk] at 300 K. Cond-mat.supr-con, 1, 2. https://doi.org/10.48550/arXiv.cond-mat/0108085

[46] Ihara, H., Sekita, Y., Tateai, F., Khan, N.A., Ishida, K., Harashima, E., Kojima, T., Yamamoto, H., Tanaka, K., Tanaka, Y., Terada, N. and Obara, H. (1999). Superconducting properties of Cu/sub 1-x/Tl/sub x/-1223 [Cu/sub 1-x/Tl/sub x/(Ba,Sr)/sub 2/Ca/sub 2/Cu/sub 3/O/sub 10-y/] thin films. IEEE Trans. Appl. Supercond. 9, 1551. https://doi.org/10.1109/77.784690.

[47] Khan, N. A., Sekita, Y., Tateai, F., Kojima, T., Ishida, K., Terada, N., & Ihara, H. (1999). Preparation of biaxially oriented TlCu-1234 thin films. Physica C: Superconductivity, 320, 39. https://doi.org/10.1016/S0921-4534(99)00294-4

[48] Awad, R., Abou Aly, A. I., Mohammed, N. H., Motaweh, H. A., & El-Said Bakeer, D. (2014). Physical and mechanical properties of $GdBa_2Cu_3O_{7-\delta}$ added with nanosized $CoFe_2O_4$. Journal of Superconductivity and Novel Magnetism, 27, 1757. https://doi.org/10.1007/s10948-014-2509-0

[49] Xu, Y., Hu, A., Xu, C., Sakai, N., Hirabayashi, I. and M. Izumi. (2008). Effect of ZrO_2 and ZnO nanoparticles inclusions on superconductive properties of the melt-processed $GdBa_2Cu_3O_{7-\delta}$ bulk superconductor. Physica C, 468,1363. https://doi.org/10.1016/j.physc.2008.05.056.

[50] Xu, C., Hu, A., Ichihara, M., Sakai, N., Hirabayashi, I. and Izumi, M. (2007). Enhanced flux pinning of air-processed Gd123 by doping ZrO_2 nanoparticles. Physica C, 460–462 ,1341. https://doi.org/10.1016/j.physc.2007.04.168.

[51] Xu, C., Hu, A., Sakai, N., Izumi, M.and Hirabayashi, I. (2006). Flux pinning properties and superconductivity of Gd-123 superconductor with addition of nanosized SnO_2/ZrO_2 particles. Physica C, 445–448 ,357. https://doi.org/10.1016/j.physc.2006.04.082.

[52] Zhang, Y.F., Izumi, M., Li, Y.J., Murakami, M., Gao, T., Liu, Y.S. and Li., P.L. (2011). Enhanced JC in air-processed $GdBa_2Cu_3O_{7-\delta}$ superconductor bulk grown by the additions of nano-particles. Physica C, 471 ,840. https://doi.org/10.1016/j.physc.2011.05.069.

[53] Xu, Y., Izumi, M., Zhang, Y.F. and Kimura, Y. (2009). Enhancement of critical current density in Gd123 bulk superconductor doped with magnetic powder. Physica C, 469 ,1215. https://doi.org/10.1016/j.physc.2009.05.020.

[54] Zhang, Y.F., Izumi, M., Xu, Y., Gao, T. and Kimura, Y. (2010). Enhanced performance in bulk superconductor $GdBa_2Cu_3O_{7-}$ with additions of $-Fe_2O_3$ particles. J. Phys. Conf. Ser. 234 ,012052. https://doi.org/10.1088/1742-6596/234/1/012052.

[55] Xu, Y., Izumi, M., Tsuzuki, K., Zhang, Y., Xu, C., Murakami, M., Sakai, N.and Hirabayashi, I. (2009). Flux pinning properties in a $GdBa_2Cu_3O_{7-\delta}$ bulk superconductor with the addition of magnetic alloy particles. Supercond. Sci. Technol. 22 ,095009. https://doi.org/10.1088/0953-2048/22/9/095009 .

[56] Baker, S. N. and Baker, G. A. (2010). Luminescent carbon nanodots: emergent nanolights. Angew. Chem., Int. Ed., 49, 6726. https://doi.org/10.1002/anie.200906623.

[57] Mukai, K. (2014). Semiconductor quantum dots for future optical applications. JNN, 14, 2148. https://doi.org/10.1166/jnn.2014.8608.

[58] Yeoh, W. K., Horvat, J., Dou, S. X. and Munroe, P. (2005). Effect of carbon nanotube size on superconductivity properties of MgB_2. IEEE Trans. Appl. Supercond., 15, 3284. https://doi.org/10.1109/tasc.2005.848853 .

[59] Serrano, G., Serquis, A., Dou, S. X., Soltanian, S., Civale, L., Maiorov, B., Holesinger, T. G., Balakirev, F. and Jaime, M. (2008). SiC and carbon nanotube distinctive effects on the superconducting properties of bulk MgB_2. J. Appl. Phys., 103, 023907. https://doi.org/10.1063/1.2832463.

[60] Anas, M., Ebrahim, S., Eldeen, I.G., Awad, R and Abou-Aly, A.I. (2017). Effect of single and multi-wall carbon nanotubes on the mechanical properties of Gd-123 superconducting phase. Chem. Phys. Lett., 686 ,34. https://doi.org/10.1016/j.cplett.2017.08.016.

[61] Çiçek, Ö and Yakinci, K. (2020). Enhanced superconducting properties of multi-wall carbon nanotubes added YBCO-123 Superconducting System. J. Mol. Struct., 1211, 128089. https://doi.org/10.1016/j.molstruc.2020.128089.

[62] Hannachi, E., Almessiere, M.A., Slimani, Y.,.Baykal, A. and Ben Azzouz, F. (2020). AC susceptibility investigation of YBCO superconductor added by carbon nanotubes, J. Alloys Compd., 812, 152150. https://doi.org/10.1016/j.jallcom.2019.152150.

[63] Elsabawy, K. M., Fallatah, A.M. and Owidah, Z.O. (2020). Nano-platinum additives ball milled with hollow carbon spheres for mechanical tensile promotion of 2212- Pb $_{1+x}$(HCNs/ Pt)$_x$BiSr$_2$CaCu$_2$O$_8$ superconductor. SN Appl. Sci., 3, 408. https://doi.org/10.1007/s42452-021-04432-8.

[64] Anas, M., El-Shorbagy, G.A., Abou-Aly, A. I. and A. Khalaf .(2022) .Synthesis, characterization and activation energy of Nano-(GO)x/(Cu,Tl)-1234 superconducting composites, J. Low Temp. Phys., 206, 210. https://doi.org/10.1007/s10909-021-02646-z.

[65] Sudesh, Das, S., Bernhard, C. and Varma, G.D. (2015). Effect of combined addition of graphene oxide and citric acid on superconducting properties of MgB$_2$. Physica C Supercond., 509, 49. https://doi.org/10.1016/j.physc.2014.12.005.

[66] Kong, W., Kongb, I., Kechikc, M.M.A.and Abd-Shukord, R. (2018). Effect of graphene addition on the transport critical current density of bulk (Tl$_{0.85}$ Cr$_{0.15}$) Sr$_2$CaCu$_2$O$_{7-\delta}$ superconductor. Mater. Today, 5, 3176. https://doi.org/10.1016/j.matpr.2018.01.125.

[67] Sahoo, B., Routray, K.L, D. Samal and Behera, D. (2019). Effect of artificial pinning centers on YBCO high temperature superconductor through substitution of graphene nano-platelets. Mater. Chem. Phys. 223 ,784. https://doi.org/10.1016/j.matchemphys.2018.11.048.

[68] Mohammed, N., Mahmoud, S., Abdeen, W. and Hasebbo, M. (2019). Influence of nano-Ag addition on phase formation and excess conductivity analysis of (CU$_{0.5}$TL$_{0.5}$)-1223 superconducting phase, BAU Journal-Science and Technology, 1, 6. https://doi.org/10.54729/2959-331X.1007.

[69] Khan, A.A., Sohail, M., Rahim, M., Mumtaz, M.and Nasir Khan, M (2020), Frequency and temperature dependent dielectric constant of (Ag)x/ CuTl-1223 nanoparticles-superconductor composites. J. Alloys Compd., 825 ,154138. https://doi.org/10.1016/j.jallcom.2020.154138.

[70] Abdeen, W., Mohammed, N.H., Awad, R., Mahmoud, S.A. and Hasebbo, M. (2013). Influence of Nano-Ag addition on phase formation and electrical properties of (Cu 0.5 Tl 0.5)-1223 superconducting phase. J. Supercond. Nov. Magn. 26 ,623. https://doi.org/10.1007/s10948-012-1803-y.

[71] Ali, L., Mumtaz, M., Ali , I., Waqee-ur-Rehman, M.and Abdul Jabbar (2017). Metallic Cu nanoparticles added to Cu$_{0.5}$ Tl$_{0.5}$ Ba$_2$Ca$_2$Cu$_3$O$_{10-\delta}$ superconductor, 10948, 017-4229-8. https://doi.org/10.1007/s10948-017-4229-8.

[72] Rahim, M., Amir Durrania, M., Mumtaz, M., Sohail, M., Qasima, M., Nasir Khan, M.. (2020). Dielectric response of (M)z/CuTl-1223 (M=Co, Cr) nanoparticle superconductor composites. Physica C Supercond, 570 ,1353601. https://doi.org/10.1016/j.physc.2020.1353601.

[73] Habanjar, K., El Haj Hassan, F. and Awad, R. (2019). Effect of BaFe$_{12}$O$_{19}$ nanoparticles addition on (Bi,Pb)-2223 superconducting phase. MAS, 13, 4. https://doi.org/10.5539/mas.v13n4p61.

[74] Rekaby, M. (2020). Dielectric response and Cole–Cole plot analysis for (Zn$_{0.91}$ Mn$_{0.03}$Co$_{0.06}$O)x/Cu$_{0.5}$Tl$_{0.5}$Ba$_2$Ca$_2$Cu$_3$O1$_{0-\delta}$ diluted magnetic

semiconductor/superconductor composites. Appl. Phys. A., 126, 664. https://doi.org/10.1007/s00339-020-03849-z.

[75] Abou-Aly, A., Ibrahim, I, Mohammed, N and Rekaby, M. (2020). Dielectric properties of $Cu_{0.5}$ $Tl_{0.5}$ $Ba_2Ca_2Cu_3O_{10-\delta}$ superconductor added with nano-Fe_2O_3, BAU Journal-Science and Technology,1, 8. https://doi.org/10.54729/2959-331X.1022.

[76] Albiss, B.A., Obaidat, I.M., Gharaibeh, M., Ghamlouche, H. and Obeidat, S.M. (2010) . Impact of addition of magnetic nanoparticles on vortex pinning and microstructure properties of Bi–Sr–Ca–Cu–O superconductor. Solid State Commun., 150, 1542. https://doi.org/10.1016/j.ssc.2010.06.001.

[77] Baqi, A. S., Abed, N. S.and Fathi, S. J. (2022). Study the effects of MgO nanoparticle addition on superconducting characteristics of $Bi_{1.6}$ $Ag_{0.4}$ $Sr_{1.9}$ $Ba_{0.1}$ $Ca_2Cu_3O_{10+\delta}$ system. J. Ovonic Res.,18, 273. https://doi.org/10.15251/JOR.2022.182.273.

[78] Wan, X., Sun, Y., Song, W., Wang, K., Jiang, L. and Du, J. (1998). Enhanced flux pinning of Bi-2223/Ag tapes with nano-MgO particles addition. Phys. C: Supercond., 307 ,46. https://doi.org/10.1016/S0921-4534(98)00400-6.

[79] N.A. Hamid, M.Y. Abd Rahman, N.F. Shamsudin. (2011). Mechanical and superconducting properties of nanosize MgO added dip-coated $Bi_2Sr_2CaCu_2O_8$ superconducting tape. Nat. Sci. 3 ,484. https://doi.org/10.4236/ns.2011.36067.

[80] Abou-Aly, A.I., Abdel Gawad, M.M.H., Awad, R. and G-Eldeen, I. (2011). Improving the physical properties of (Bi, Pb)-2223 phase by SnO_2 nano-particles addition. J. Supercond. Nov. Magn. 24 ,2077. https://doi.org/10.1007/s10948-011-1171-z.

[81] Jia, Z.Y., Tang, H., Yang, Z.Q., Xing, Y.T., Wang, Y.Z. and Qiao, G.W. (2000). Effects of nano-ZrO_2 particles on the superconductivity of Pb-doped BSCCO. Phys. C: Supercond., 337 ,130. https://doi.org/10.1016/S0921-4534(00)00072-1.

[82] Annabi, M., chirgui, A.M, Ben Azzouz, F., Zouaoui, M. and Ben Salem, M. (2004). Addition of nanometer Al_2O_3 during the final processing of (Bi,Pb)-2223 superconductors. Phys. C: Supercond. Appl., 405 , 25. https://doi.org/10.1016/j.physc.2004.01.012.

[83] Sengupta, S., Todt, V.R., Kostic, P., Chen, Y.L., Lanagan, M.T. and Goretta, K.C. (1996). Flux pinning in $TlBa_2Ca_2Cu_3O_x$ through addition of nanophase Al_2O_3. Phys. C: Supercond. Appl., 264, 34. https://doi.org/10.1016/0921-4534(96)00191-8.

[84] Awad, R. (2008). Study of the influence of MgO nano-oxide addition on the electrical and mechanical properties of $(Cu_{0.25}Tl_{0.75})$-123 superconducting phase. J. Supercond. Nov. Magn. 21 ,461. https://doi.org/10.1007/s10948-008-0385-1.

[85] Elokr, M.M. Awad, R., El-Ghany, A.A., Shama, A.A. and El-wanis, A.A. (2011). Effect of nno-sized ZnO on the physical properties of $(Cu_{0.5}Tl_{0.25}Pb_{0.25})Ba_2Ca_2Cu_3O_{10-\delta}$. J. Supercond. Nov. Magn., 24 ,1345. https://doi.org/10.1007/s10948-010-0831-8.

[86] Mohammed, N.H., Abou-Aly, A.I., Ibrahim, I.H., Awad, R. and Rekaby, M. (2009). Mechanical properties of $(Cu_{0.5}Tl_{0.5})$-1223 added by nano-SnO_2. J. Alloys Compd. 486 ,733. https://doi.org/10.1016/j.jallcom.2009.07.034.

[87] Mohammed, N.H. , Abou-Aly, A.I., Ibrahim, I.H., Awad, R. and Rekaby, M. (2011). Effect of nano-oxides addition on the mechanical properties of $(Cu_{0.5}Tl_{0.5})$-1223 Phase. J. Supercond. Nov. Magn. 24 ,1463. https://doi.org/10.1007/s10948-010-0853-2.

[88] Mohammed, N.H. , Abou-Aly, A.I., Awad, R., Ibrahim, I.H., Roumie, M. and Rekaby, M. (2013) . Mechanical and electrical properties of $(Cu_{0.5}Tl_{0.5})$-1223 phase added with nano-Fe_2O_3. J. Low Temp Phys. 172, 234. https://doi.org/10.1007/s10909-013-0867-9.

[89] Matar, M., Basma, H., Abbas, S. and Awad, R. (2022). Thermal and mechanical investigations of(Bi,Pb)-2212

DOI: 10.62184/acj.jacj1000202425

superconductor added with different oxide nanoparticles. Preprint. https://doi.org/10.1520/MPC20230046

[90] Shalaby, M.S., Hamed, M.H., Yousif, N.M and Hashem, H.M. (2021). The impact of the addition of Bi_2Te_3 nanoparticles on the structural and the magnetic properties of the Bi-2223 high-T_c superconductor. Ceram. Int. 47, 25236. https://doi.org/10.1016/j.ceramint.2021.05.244.

[91] Akbar, A., Imaduddin, A., Humaidi, S. and Nugraha, H. (2021). Effect of $BaCO_3$ addition on critical temperature of Bi-Pb-Sr- Ca-Cu-O superconductor. J. Phys. Conf. Ser., 1882 ,012014. https://doi.org/10.1088/1742-6596/1882/1/012014.